The decays were found to be strongly curved, and the fit to the initial part yielded a rate coefficient of $\sim 7 \times 10^{-11}$ cm^3 s^{-1}, approximately 15% higher than when the "true" background was used. On the other hand, using the pretrigger background resulted in a rate coefficient identical with that obtained when the boxcar delay was extended so that only CH_3S was detected. Product formation is a potential reason for the higher value of the rate coefficient obtained by Balla et al.,[15] depending on the exact wavelength and boxcar delay they used.

Implications for Atmospheric Chemistry. The upper limit for the $CH_3S + O_2$ reaction rate coefficient determined here is an order of magnitude lower than previous estimates. We still cannot rule out this reaction in the atmosphere, though. O_2 has a mole fraction of 0.21, and this implies a loss rate for CH_3S of ≤ 15 s^{-1} in the lower troposphere. Even though the NO_2 reaction rate coefficient is 6×10^{-11} cm^3 s^{-1}, the maximum NO_2 mixing ratio observed in the background troposphere is around 100–300 ppt ($(2.5–7.5) \times 10^9$ cm^{-3}),[18] giving a loss rate of 0.2–0.5 s^{-1}. In the marine boundary layer, where most of the atmospheric CH_3S oxidation occurs, the NO_2 concentration may be as low as 10 ppt (3×10^8 cm^{-3}). The upper limit for the O_2 reaction is therefore still 3 orders of magnitude higher than we need to rule this reaction out.

Our results indicate that CH_3S and O_2 do not form a strongly bound adduct and that such an adduct, if formed at all, does not react rapidly with O_2. Therefore, the loss rate for CH_3S which we observe will correspond to the actual loss rate in the atmosphere, provided the adduct does not react with other trace molecules, such as NO, NO_2, or O_3, substantially faster than CH_3S does.

$$CH_3S(O_2) + NO \rightarrow CH_3SO + NO_2$$
$$CH_3S(O_2) + NO_2 \rightarrow \text{products}$$
$$CH_3S(O_2) + O_3 \rightarrow CH_3SO + 2O_2$$

The most pressing problem remains the identification of the mechanisms by which CH_3S is converted to SO_2 and MSA at low NO_x. Simultaneous measurements of the DMS flux and SO_2 in the marine troposphere suggest that SO_2 is the major product of DMS oxidation, maybe accounting for 90% of the oxidized sulfur.[46] However, the laboratory studies have consistently shown reduced SO_2 yields and a predominance of MSA. It is not clear whether this reflects the mode of attack on CH_3S or subsequent reactions of radicals with the precursor.[9,13] Our experiments show that oxidation of CH_3S to CH_3SO and presumably CH_3SO_2 occurs rapidly in the presence of NO_2, and Hatakeyama et al. have recently shown that if ^{18}O-labeled NO_2 is used, some of the SO_2 produced contains ^{18}O,[47] indicating the importance of the $CH_3S + NO_2$ reaction in the production of SO_2 in chambers. The formation of MSA, CH_3SO_3H, could also follow CH_3SO_2 production.[43] However, under atmospheric conditions of low NO_2 different considerations may apply, and an oxidation chain initiated by $CH_3S + O_2$ could give a different product distribution. These questions can only be resolved by a thorough study of CH_3SO and CH_3SO_2 chemistry and more mechanistic information on the $CH_3S + O_2$ reaction.

Acknowledgment. This work was supported by NOAA as part of the National Acid Precipitation Assessment Program. We are grateful to D. Fahey for analyzing the NO mixture, A. Wahner for writing the data handling programs, and J. Smith for help with the design and construction of the detection optics.

(46) Saltzman, E. S.; Savoie, D. L.; Zika, R. G.; Prospero, J. M. *J. Geophys. Res.* **1983**, *88*, 10897.
(47) Hatakeyama, S. In *Proceedings of 194th ACS Meeting, New Orleans, 1987*, in press.
(48) Tyndall, G. S.; Ravishankara, A. R. In *Proceedings of the 194th ACS Meeting, New Orleans, 1987*, in press.

Ab Initio Study of the Addition Reaction of the Methyl Radical to Ethylene and Formaldehyde

Carlos Gonzalez, Carlos Sosa,[†] and H. Bernhard Schlegel*[,‡]

Department of Chemistry, Wayne State University, Detroit, Michigan 48202 *(Received: June 17, 1988; In Final Form: September 28, 1988)*

A detailed study of the potential energy surfaces for methyl radical plus ethylene and methyl radical plus formaldehyde has been carried out with the 3-21G and 6-31G* basis sets at the Hartree–Fock level. Heats of reaction and barrier heights have been computed with the Møller–Plesset perturbation theory up to the fourth order with and without annihilation of spin contamination. The results of the calculations indicate the formation of an early transition state with reactant-like structure for both reactions. In the case of methyl radical plus ethylene, spin annihilation lowers the barrier height by 7 kcal/mol, while in the reaction between methyl radical and formaldehyde the barrier is lowered by 6 kcal/mol when spin annihilation is considered. A comparison between the calculated and experimental values of the barrier height for the methyl addition to ethylene (6.9 kcal/mol vs 7.9 kcal/mol) and formaldehyde (6.3 kcal/mol vs 6.8 kcal/mol) indicates very good agreement between theory and experiment.

Introduction

Although radical additions to double bonds have been extensively studied experimentally,[1,2] there is still some controversy about the nature of the transition states. While experimental data lead to the conclusion that these reactions have tight transition states with productlike structures,[3–5] the low activation energies and high exothermicities of these reactions would suggest early, reactant-like transition states.[1,6,7]

[†] Present address: Quantum Theory Project, University of Florida, Gainesville, FL 32605.
[‡] Camile and Henry Dreyfus Teacher–Scholar.

(1) Kerr, J. A.; Parsonage, M. J. *Evaluated Kinetic Data on Gas Addition Reactions: Reaction of Atoms and Radicals with Alkenes, Alkynes, and Aromatic Compounds*; Butterworths: London, 1972.
(2) Kerr, J. A. *Free Radicals*; Kochi, J., Ed.; Wiley: New York, 1972; Vol. 1.
(3) Benson, S. W.; O'Neal, H. E. *NBS Stand. Ref. Ser.* **1970**, *No. 21*.
(4) Frey, H. M.; Walsh, R. R. *Chem. Rev.* **1969**, *69*, 103.
(5) Kerr, J. A.; Lloyd, A. C. *Q. Rev. Chem. Soc.* **1968**, *22*, 549.

0022-3654/89/2093-2435$01.50/0 © 1989 American Chemical Society

The addition of methyl radical is one of the simplest models for free-radical polymerization. Experimental studies indicate that these reactions are exothermic and exhibit a low activation energy.[2] Early theoretical studies[8-14] were limited primarily to semiempirical methods and small basis set ab initio calculations at the UHF level. Recent ab initio calculations include studies of regioselectivity and substituent effects.[15]

The $CH_3 + CH_2O \rightleftharpoons CH_3CH_2O$ reaction is an important process in combustion chemistry and in atmospheric chemistry.[16-20] Gas-phase studies indicate a barrier of 20–22 kcal/mol for the decomposition of ethoxy radical into methyl radical and formaldehyde, and a barrier of 6.8 kcal/mol for the addition reaction.[21-23] High-level theoretical calculations have been carried out on this reaction as part of a study on the $OH + C_2H_4$ system.[24,25]

In previous studies of radical additions to multiple bonds,[26] we have noted that UHF calculations of the transition states have substantial spin contamination. Under such circumstances, barriers can be up to 10 kcal/mol too high when correlation corrections are calculated by unrestricted Møller–Plesset perturbation theory. When spin projection is used in conjunction with perturbative correlation corrections, the heights and positions of the barriers are improved considerably. In the present paper, these techniques are used to study the barrier heights and the shape of the potential energy curves along the reaction paths for methyl radical addition to ethylene and to formaldehyde.

Method

Ab initio molecular orbital calculations were performed with the Gaussian 82 and 86 systems of programs.[27] Geometries of reactants, products, and transition states were fully optimized at the Hartree–Fock level with analytical gradient methods[28] using split-valence (3-21G)[29] and split-valence plus polarization (6-31G*)[30] basis sets. Several points were calculated along the reaction paths for the methyl radical addition to ethylene and formaldehyde by fixing the methyl–reactant distance, R(C–C), and minimizing the energy with respect to all other parameters. Electron correlation was calculated with fourth-order Møller–Plesset perturbation theory in the space of single, double, and quadruple excitations (MP4SDQ, frozen core) with and without annihilation of the largest spin contaminant. Finally, vibrational frequencies and zero-point energies were obtained from analytical second derivatives[31] calculated at the HF/3-21G level.

In the region of the transition structure, the unrestricted Hartree–Fock calculations suffer serious problems with spin contamination, i.e., $\langle\Psi_0|\hat{S}^2|\Psi_0\rangle \neq s(s+1)$. Inclusion of MP$n$ correlation corrections in the calculation of $\hat{S}^2$, e.g., $\langle\Psi_0|\hat{S}^2|\Psi_0 + \Psi_1\rangle$, $\langle\Psi_0|\hat{S}^2|\Psi_0 + \Psi_1 + \Psi_2\rangle$, etc., does not improve the situation significantly. However, the unwanted spin contaminants can be removed by using the Löwdin spin projection operator.[32] This series converges rapidly, and only the largest two or three spin contaminants need to be annihilated. The projected Hartree–Fock energy can be written as

$$E_{\mathrm{PUHF}} = \langle\Psi_0|\hat{H}\hat{P}_s|\Psi_0\rangle / \langle\Psi_0|\hat{P}_s|\Psi_0\rangle = \langle\Psi_0|\hat{H}|\Psi_0\rangle + \langle\Psi_0|\hat{H}|\tilde{\Psi}_1\rangle = E_{\mathrm{UHF}} + \Delta E_{\mathrm{PUHF}} \quad (1)$$

where $\tilde{\Psi}_1$ contains all of the contributions from the single and double excitations

$$\tilde{\Psi}_1 = \sum_i^{s,d} \psi_i \langle\psi_i|\hat{P}_s|\Psi_0\rangle / \langle\Psi_0|\hat{P}_s|\Psi_0\rangle \quad (2)$$

and the Löwdin spin projection operator is given by

$$\hat{P}_s = \prod_{k\neq s} \frac{\hat{S}^2 - k(k+1)}{s(s+1) - k(k+1)} \quad (3)$$

Since electron correlation energies with spin projection are difficult to calculate directly, two approximations are made: (a) Only single and double excitations are considered for the spin projection

TABLE I: Total Energies for the $CH_3 + C_2H_4$ System[a]

level	reactant	transition state	product
UHF/3-21G	−116.943 591	−116.932 881	−116.982 491
UMP2/3-21G	−117.198 205	−117.177 491	−117.237 076
UMP3/3-21G	−117.227 408	−117.207 692	−117.266 342
UMP4/3-21G	−117.237 220	−117.218 751	−117.274 594
$\langle\Psi_0\|\hat{S}^2\|\Psi_0\rangle$	0.761 90	1.026 02	0.762 36
$\langle\Psi_0\|\hat{S}^2\|\Psi_0 + \Psi_1\rangle$	0.758 18	0.989 03	0.757 94
$\langle\Psi_0\|\hat{S}^2\|\Psi_0 + \Psi_1 + \Psi_2\rangle$	0.755 29	0.936 37	0.754 74
PUHF/3-21G	−116.946 115	−116.951 052	−116.985 306
PMP2/3-21G	−117.199 940	−117.193 273	−117.238 997
PMP3/3-21G	−117.228 533	−117.220 048	−117.267 565
PMP4/3-21G	−117.238 344	−117.231 107	−117.275 818
$\langle\Psi_0\|\hat{S}^2\hat{P}_s\|\Psi_0\rangle$	0.750 00	0.750 00	0.750 00
UHF/6-31G*	−117.590 620	−117.575 692	−117.631 434
UMP2/6-31G*	−117.953 090	−117.930 115	−117.999 787
UMP3/6-31G*	−117.989 992	−117.967 990	−118.035 593
UMP4/6-31G*	−117.998 306	−117.977 966	−118.042 589
$\langle\Psi_0\|\hat{S}^2\|\Psi_0\rangle$	0.761 80	1.028 64	0.762 37
$\langle\Psi_0\|\hat{S}^2\|\Psi_0 + \Psi_1\rangle$	0.757 63	0.991 32	0.754 11
$\langle\Psi_0\|\hat{S}^2\|\Psi_0 + \Psi_1 + \Psi_2\rangle$	0.754 62	0.937 54	0.753 09
PUHF/6-31G*	−117.593 695	−117.594 679	−117.634 623
PMP2/6-31G*	−117.954 407	−117.946 610	−118.001 837
PMP3/6-31G*	−117.991 199	−117.980 863	−118.036 820
PMP4/6-31G*	−117.999 513	−117.990 834	−118.043 816
$\langle\Psi_0\|\hat{S}^2\hat{P}_s\|\Psi_0\rangle$	0.750 00	0.750 00	0.750 00

[a] Total energies in atomic units; structures optimized at the UHF/3-21G and UHF/6-31G* levels.

(6) Nonhebel, D. C.; Walton, J. C. *Free Radical Chemistry*; Cambridge University Press: Cambridge, 1974; p 225.
(7) Tedder, J. M.; Walton, J. C. *Adv. Phys. Org. Chem.* **1978**, *16*, 51.
(8) Basilevsky, M. V.; Chelenov, I. E. *Theor. Chim. Acta* **1969**, *15*, 174.
(9) Hoyland, J. R. *Theor. Chim. Acta* **1971**, *22*, 229.
(10) Dewar, M. J. S.; Olivella, S. *J. Am. Chem. Soc.* **1978**, *100*, 5290.
(11) Gey, E.; Kuhnel, W. *Collect. Czech. Chem. Commun.* **1979**, *44*, 3649.
(12) Canadell, E.; Poblet, J. M.; Olivella, S. *J. Phys. Chem.* **1983**, *87*, 424.
(13) Clark, D. T.; Scanlan, I. W.; Walton, J. C. *Chem. Phys. Lett.* **1978**, *55*, 102.
(14) Arnaud, R.; Barone, V.; Olivella, S.; Sole, A. *Chem. Phys. Lett.* **1985**, *118*, 573.
(15) Canabell, E.; Eisenstein, O.; Ohanessian, G.; Poblet, J. M. *J. Phys. Chem.* **1985**, *89*, 4856.
(16) Allara, D. L.; Mill, T.; Hendry, G. D.; Mayo, F. R. *Adv. Chem. Ser.* **1968**, *No. 76*, 40.
(17) Demerjian, K. L.; Kerr, J. A.; Calvert, J. G. *Adv. Environ. Sci. Technol.* **1974**, *4*, 1.
(18) Adamic, K.; Howard, J. A.; Ingold, K. U. *Can. J. Chem.* **1969**, *47*, 3803.
(19) Benson, S. W. *Thermochemical Kinetics*, 2nd ed.; Wiley: New York, 1976; p 239.
(20) Pate, C. T.; Finlayson, B. J.; Pitts, J. N., Jr. *J. Am. Chem. Soc.* **1974**, *96*, 6554.
(21) Batt, L.; Milne, R. T. *Int. J. Chem. Kinet.* **1977**, *9*, 549.
(22) Batt, L. *Int. J. Chem. Kinet.* **1979**, *11*, 977.
(23) Choo, K. Y.; Benson, S. W. *Int. J. Chem. Kinet.* **1981**, *13*, 833.
(24) Melius, C. F.; Binkley, J. S.; Koszykowski, M. L. 8th International Symposium on Gas Kinetics, Nottingham, England, 1984, and unpublished results.
(25) Sosa, C.; Schlegel, H. B. *J. Am. Chem. Soc.* **1987**, *109*, 4193.
(26) Sosa, C.; Schlegel, H. B. *Int. J. Quantum Chem., Quantum Chem. Symp.* **1987**, *21*, 267.
(27) Binkley, J. S.; Frisch, M. J.; DeFrees, D. J.; Raghavachari, K.; Whiteside, R. A.; Schlegel, H. B.; Fluder, E. M.; Pople, J. A. *Gaussian 82*; Carnegie-Mellon University: Pittsburgh, 1983. Binkley, J. S.; Frisch, M. J.; DeFrees, D. J.; Raghavachari, K.; Whiteside, R. A.; Schlegel, H. B.; Fox, D. J.; Martin, R. L.; Fluder, E. M.; Melius, C. F.; Kahn, L. R.; Steward, J. J. P.; Bobrowicz, F. W.; Pople, J. A. *Gaussian 86*; Carnegie-Mellon University: Pittsburgh, 1984.
(28) Schlegel, H. B. *J. Comput. Chem.* **1982**, *3*, 214.
(29) Binkley, J. S.; Pople, J. A.; Hehre, W. J. *J. Am. Chem. Soc.* **1980**, *102*, 939.
(30) Hariharan, P. C.; Pople, J. A. *Theor. Chim. Acta* **1973**, *28*, 213.
(31) Pople, J. A.; Krishnan, R.; Schlegel, H. B.; Binkley, J. S. *Int. J. Quantum Chem., Quantum. Chem. Symp.* **1979**, *13*, 225.
(32) Löwdin, P.-O. *Phys. Rev.* **1955**, *97*, 1509.

TABLE II: Total Energies for the CH_3 + CH_2O System[a]

level	reactant	transition state	product
UHF/3-21G	−152.564 434	−152.561 822	−152.616 400
UMP2/3-21G	−152.854 931	−152.828 805	−152.880 481
UMP3/3-21G	−152.867 245	−152.848 555	−152.903 288
UMP4/3-21G	−152.880 866	−152.862 787	−152.911 674
$\langle\Psi_0\|\hat{S}^2\|\Psi_0\rangle$	0.761 89	1.035 36	0.756 11
$\langle\Psi_0\|\hat{S}^2\|\Psi_0 + \Psi_1\rangle$	0.758 17	0.998 37	0.754 35
$\langle\Psi_0\|\hat{S}^2\|\Psi_0 + \Psi_1 + \Psi_2\rangle$	0.755 29	0.939 68	0.752 89
PUHF/3-21G	−152.566 956	−152.581 824	−152.617 831
PMP2/3-21G	−152.856 665	−152.846 253	−152.881 501
PMP3/3-21G	−152.868 369	−152.861 923	−152.903 966
PMP4/3-21G	−152.881 990	−152.876 156	−152.912 352
$\langle\Psi_0\|\hat{S}^2\hat{P}_s\|\Psi_0\rangle$	0.750 00	0.750 00	0.750 00
UHF/6-31G*	−153.423 934	−153.411 200	−153.460 936
UMP2/6-31G*	−153.832 184	−153.811 100	−153.856 126
UMP3/6-31G*	−153.854 731	−153.838 500	−153.887 719
UMP4/6-31G*	−153.865 451	−153.850 200	−153.895 231
$\langle\Psi_0\|\hat{S}^2\|\Psi_0\rangle$	0.761 48	0.943 08	0.757 56
$\langle\Psi_0\|\hat{S}^2\|\Psi_0 + \Psi_1\rangle$	0.757 38	0.911 71	0.754 47
$\langle\Psi_0\|\hat{S}^2\|\Psi_0 + \Psi_1 + \Psi_2\rangle$	0.754 45	0.866 34	0.752 63
PUHF/6-31G*	−153.426 972	−153.428 900	−153.464 086
PMP2/6-31G*	−153.834 138	−153.825 900	−153.857 992
PMP3/6-31G*	−153.855 911	−153.849 300	−153.888 817
PMP4/6-31G*	−153.866 631	−153.860 900	−153.896 329
$\langle\Psi_0\|\hat{S}^2\hat{P}_s\|\Psi_0\rangle$	0.750 00	0.750 00	0.750 00

[a] Total energies in atomic units; structures optimized at the UHF/3-21G and UHF/6-31G* levels.

corrections to Ψ_0. (b) The spin projection corrections, $\tilde{\Psi}_1$, are reduced by the amount already contained in the correlation corrections, Ψ_1, Ψ_2, etc. These approximations have been used successfully in previous calculations where only the largest spin contaminant was annihilated.[33,34] The approximate projected MP2, MP3, and MP4 energies used in the present calculations are

$$E_{PMP2} = E_{MP2} + \Delta E_{PUHF}\{1 - \langle\Psi_1|\tilde{\Psi}_1\rangle/\langle\tilde{\Psi}_1|\tilde{\Psi}_1\rangle\} \quad (4)$$

$$E_{PMP3} = E_{MP3} + \Delta E_{PUHF}\{1 - \langle\Psi_1 + \Psi_2|\tilde{\Psi}_1\rangle/\langle\tilde{\Psi}_1|\tilde{\Psi}_1\rangle\} \quad (5)$$

$$E_{PMP4} = E_{MP4} + \Delta E_{PUHF}\{1 - \langle\Psi_1 + \Psi_2 + \Psi_3|\tilde{\Psi}_1\rangle/\langle\tilde{\Psi}_1|\tilde{\Psi}_1\rangle\} \approx E_{MP4} + \Delta E_{PUHF}\{1 - \langle\Psi_1 + \Psi_2|\tilde{\Psi}_1\rangle/\langle\tilde{\Psi}_1|\tilde{\Psi}_1\rangle\} \quad (6)$$

Results and Discussion

Figures 1 and 2 show the optimized geometries of the transition structures and products. In general, the geometries obtained with the 3-21G and 6-31G* basis sets are quite similar. The total energies are collected in Tables I and II. The harmonic vibrational frequencies calculated at the UHF/3-21G level are presented in Table III. When compared with experiment, frequencies calculated at this level are ca. 11% too high as a result of basis set effects, lack of electron correlation, and neglect of anharmonicity. The calculated heats of reaction and barrier heights for the two methyl addition reactions are given in Table IV.

Transition Structures. The calculated transition structures (Figure 1) are quite reactant-like and are characterized by relatively large distances between the methyl radical and the unsaturated species (2.246 Å for CH_3 + C_2H_4 and 2.140 Å for CH_3 + CH_2O at the UHF/6-31G* level). Spin projection shifts these positions by only a small amount toward the reactants (see text below). The ethylene and formaldehyde fragments in the transition states are distorted by only a small amount. By contrast, the methyl radical shows significant pyramidalization. This is in keeping with the fact that the out-of-plane bending potential for methyl radical is known to be broad and shallow.[35]

Barrier Heights. Portions of the potential energy surface near the transition state are shown in Figures 3 and 4 for CH_3 + C_2H_4 and in Figures 5 and 6 for CH_3 + CH_2O. The interpolated barrier heights are given in Table IV. At the Hartree–Fock level, the barriers are in fair to poor agreement with experiment. When correlation corrections are added, the barriers are raised by 2–15 kcal/mol, making the agreement with experiment worse. Spin projection lowers the MP*n* barriers by 5–10 kcal/mol, improving

TABLE III: Vibrational Frequencies for Minima and Transition Structures for the Reactions CH_3 + CH_2CH_2 and CH_3 + CH_2O[a]

molecule	frequency, cm^{-1}
minima	
CH_3	424 (580), 1544 (1381), 1544 (1383), 3251 (3002), 3251 (3002), 3428 (3184)
C_2H_4	944 (826), 1115 (949), 1157 (943), 1165 (1023), 1387 (1236), 1522 (1242), 1640 (1444), 1842 (1623), 3238 (3026), 3305 (2989), 3371 (3103), 3403 (3106)
CH_2O	1337 (1167), 1378 (1249), 1692 (1500), 1916 (1746), 3162 (2783), 3233 (2843)
$CH_3CH_2CH_2$ (anti)	120, 263, 354, 531, 814, 926, 988, 1054, 1183, 1386, 1447, 1470, 1564, 1596, 1656, 1671, 1674, 3195, 3204, 3232, 3256, 3266, 3285, 3389
$CH_3CH_2CH_2$ (gauche)	124, 264, 401, 470, 833, 911, 1007, 1097, 1177, 1287, 1421, 1495, 1569, 1596, 1650, 1672, 1675, 3150, 3196, 3215, 3255, 3261, 3283, 3388
OCH_2CH_3	154, 352, 421 (442), 908 (873), 1000, 1071 (1067), 1203, 1397, 1504 (1342), 1577, 1631, 1659, 1670, 3201, 3210, 3230, 3270, 3281
transition structures	
$CH_3\cdots CH_2CH_2$	420*i*, 101, 251, 402, 580, 599, 853, 898, 909, 1037, 1037, 1291, 1363, 1579, 1583, 1619, 1673, 3242, 3302, 3317, 3376, 3387, 3397, 3408
$CH_3\cdots CH_2O$	321*i*, 94, 242, 515, 563, 679, 893, 1082, 1326, 1335, 1564, 1572, 1707, 3226, 3250, 3317, 3404, 3417

[a] The values in parentheses refer to experimental frequencies.

TABLE IV: Heat of Reaction and Energy Barriers for the Addition Reactions CH_3 + CH_2O and CH_3 + C_2H_4[a]

	CH_3 + CH_2CH_2		CH_3 + CH_2O	
level of calcn	energy barrier	heat of reaction	energy barrier	heat of reaction
UHF/3-21G	6.7	−24.4	1.6	−32.6
UMP2/3-21G	13.0	−24.4	16.4	−16.0
UMP3/3-21G	12.4	−24.4	11.7	−22.6
UMP4/3-21G	11.6	−23.5	11.3	−19.3
PUHF/3-21G	−3.1	−24.6	−9.3	−31.9
PMP2/3-21G	4.2	−24.5	6.5	−15.6
PMP3/3-21G	5.3	−24.5	4.0	−22.3
PMP4/3-21G	4.5	−23.5	3.7	−19.1
UHF/6-31G*	9.4	−25.6	8.0	−23.2
UMP2/6-31G*	14.4	−29.3	13.2	−15.0
UMP3/6-31G*	13.8	−28.6	10.2	−20.7
UMP4/6-31G*	12.8	−27.8	9.6	−18.7
PUHF/6-31G*	−0.6	−25.7	−1.2	−23.3
PMP2/6-31G*	4.9	−29.8	5.2	−15.0
PMP3/6-31G*	6.5	−28.6	4.1	−20.6
PMP4/6-31G*	5.4	−27.8	3.6	−18.6
ΔZPE/3-21G	1.5		2.7	
theor barrier	6.9		6.3	
exptl barrier	7.9		6.8	

[a] In kilocalories per mole, at 0 K.

(33) Sosa, C.; Schlegel, H. B. *Int. J. Quantum Chem.* **1986**, *29*, 1001; *30*, 155.

(34) Schlegel, H. B. *J. Chem. Phys.* **1986**, *84*, 4530.

(35) Yamada, C.; Hirota, E.; Kawaguchi, K. J. *J. Chem. Phys.* **1981**, *75*, 5256. Riveros, J. M. *J. Chem. Phys.* **1969**, *51*, 1269. Chipman, D. M. *J. Chem. Phys.* **1983**, *78*, 3112.

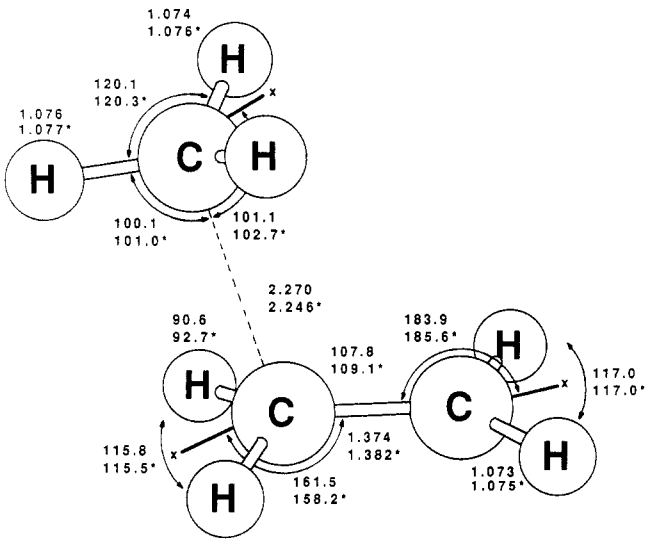

(a)

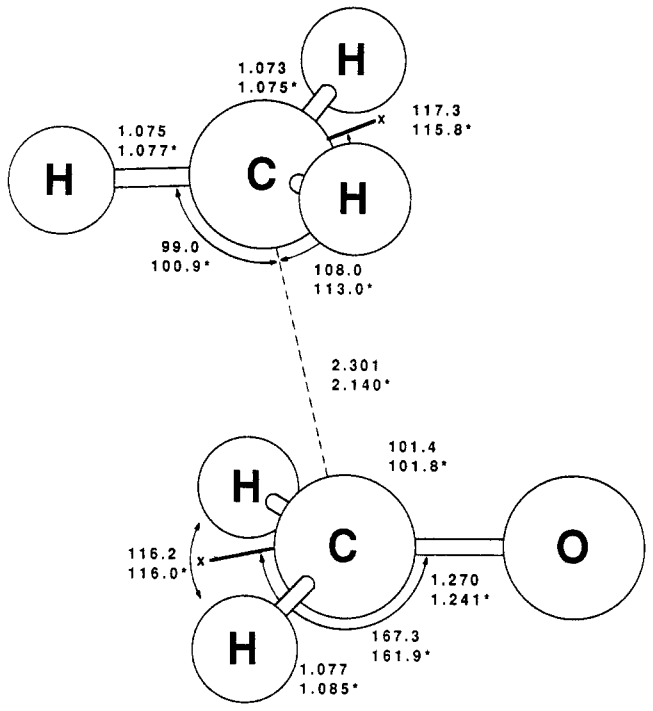

(b)

Figure 1. Transition structures for (a) $CH_3 + C_2H_4$ and (b) $CH_3 + CH_2O$ calculated at the UHF/3-21G level (no superscript) and at the UHF/6-31G* level (asterisk). Bond lengths are in angstroms and angles in degrees.

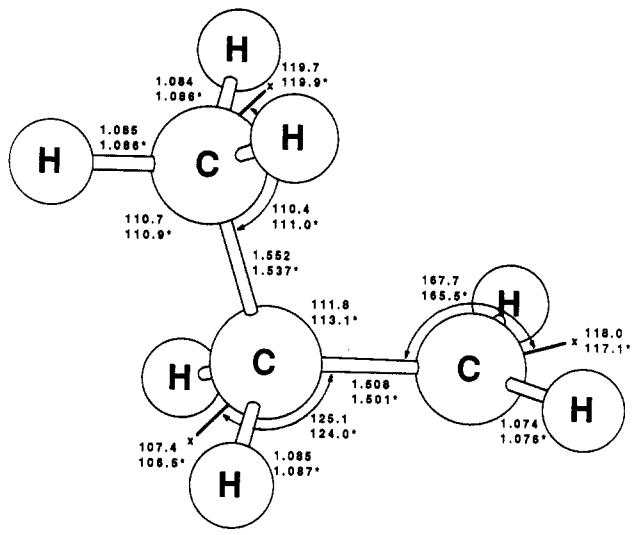

(a)

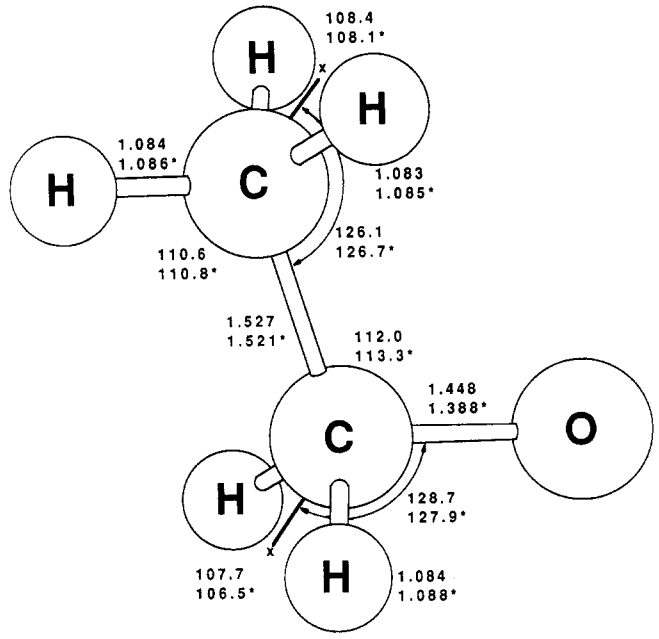

(b)

Figure 2. Optimized geometries for (a) C_3H_7 and (b) C_2H_5O calculated at the UHF/3-21G level (no superscript) and at the UHF/6-31G* level (asterisk). Bond lengths are in angstroms and angles in degrees.

the agreement in each case. As can be seen from Figures 3–6, spin projection also shifts the transition states by ca. 0.05 Å toward the reactants.[36] When zero-point energy is included, the vibrationally adiabatic barrier at the PMP4/6-31G* level is 6.9 kcal/mol for $CH_3 + C_2H_4$ compared to the experimental activation energy of 7.9 kcal/mol.[2] For $CH_3 + CH_2O$, the calculated vibrationally adiabatic barrier is 6.3 kcal/mol compared to the experimental activation energy of 6.8 kcal/mol.[23] Spin projection and correlation corrections lower the imaginary frequencies at the transition state to approximately $354i$ cm^{-1} for $CH_3 + C_2H_4$ and $271i$ cm^{-1} for $CH_3 + CH_2O$ at the PMP4/3-21G level (using the HF/3-21G geometry and calculating the force constant along the HF/3-21G normal mode by numerical differentiation at the PMP4/3-21G level).

Products. The CH_2 group in propyl radical is slightly nonplanar in the anti conformation shown in Figure 2a and in the gauche conformation (not shown). The anti conformation is slightly more stable (ca. 0.05 kcal/mol at the UHF/3-21G level), but the rotational barrier between these two conformers is extremely low (ca. 0.1 kcal/mol).[37-39] Thus, the CH_2 group is calculated to be a nearly free rotor, in agreement with experiment.[40] As indicated in Table III, a low-frequency β-CH stretch is predicted to be present for the gauche conformation, but absent in the anti conformation. This suggests that the gauche structure has been seen in recent experimental matrix isolation vibrational spectra.[41]

(36) Barriers calculated at the UHF-optimized transition states are ca. 0.5 kcal/mol lower.

(37) Pacansky, J.; Dupuis, M. *J. Chem. Phys.* **1979**, *71*, 2095.
(38) Krusic, P. J.; Meakin, P.; Jeeson, J. P. *J. Phys. Chem.* **1971**, *75*, 3438.
(39) Claxton, T. A.; Graham, A. M. *J. Chem. Soc., Faraday Trans.* **1988**, *84*, 121.
(40) Adrian, J. F.; Cochran, E. L.; Bowers, V. A. *J. Chem. Phys.* **1971**, *59*, 3946.

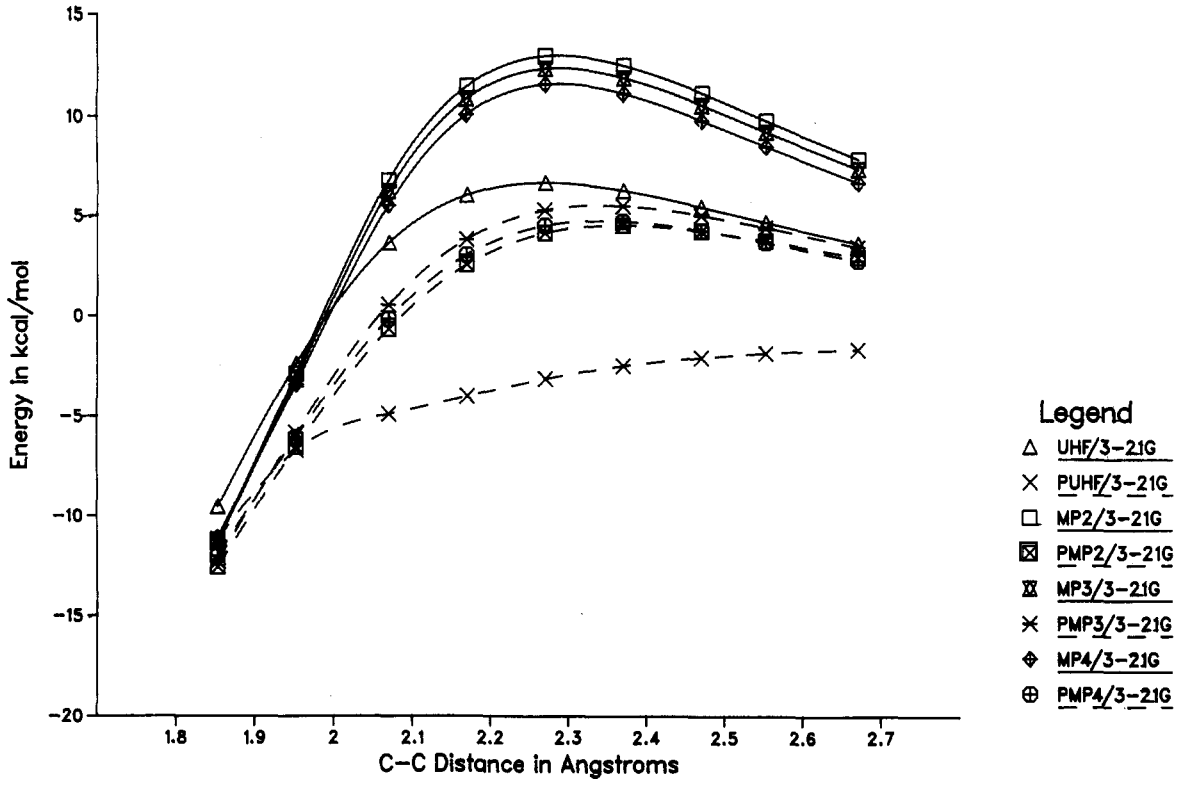

Figure 3. Potential energy profile along an approximate reaction path for methyl radical addition to ethylene computed with the 3-21G basis set.

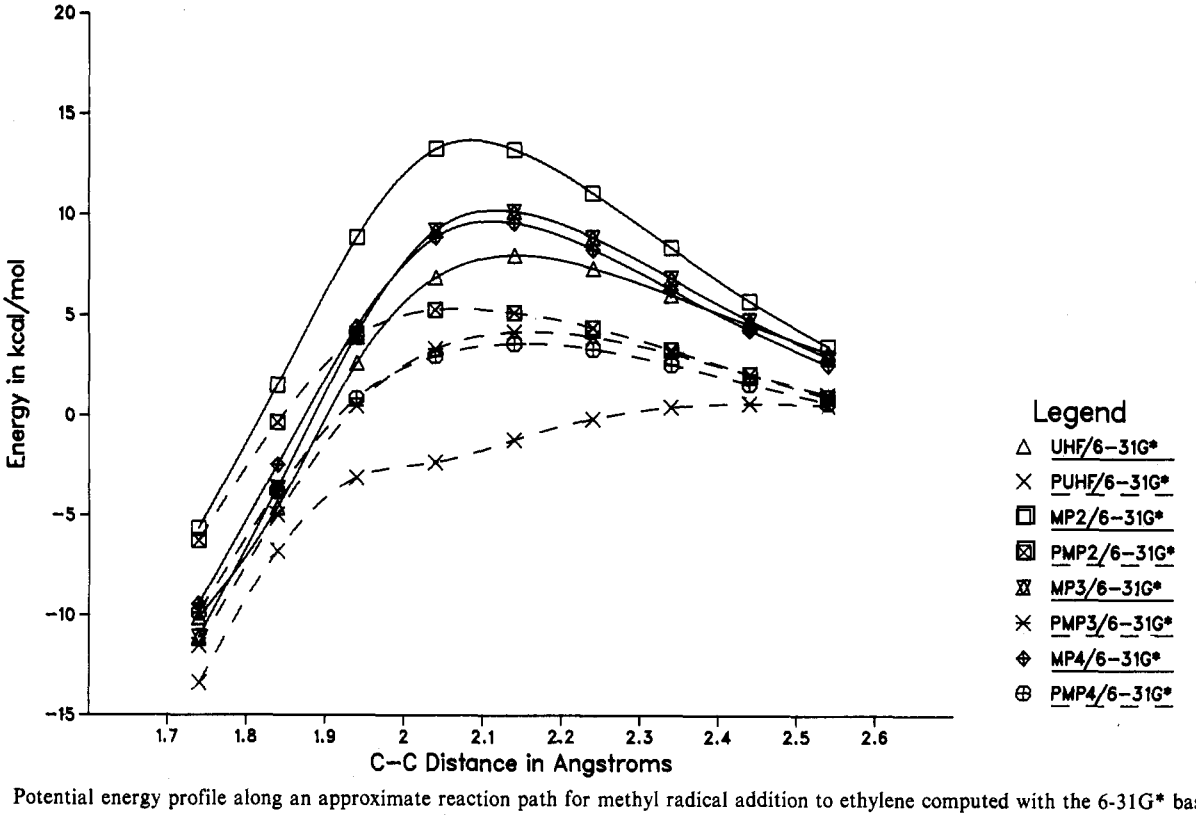

Figure 4. Potential energy profile along an approximate reaction path for methyl radical addition to ethylene computed with the 6-31G* basis set.

The calculated structure of ethoxy radical has been discussed previously.[25] Like methoxy radical,[42] ethoxy has a $^2A'$ ground state.

Heats of Reaction. The experimental heats of formation at 0 K are 14.6 kcal/mol for C_2H_4,[43] −26.8 kcal/mol for CH_2O,[43] 35.6 kcal/mol for CH_3,[43] 24.7 kcal/mol for C_3H_7,[44] and −0.15 kcal/mol for C_2H_5O.[21,22] For $CH_3 + C_2H_4$, this yields $\Delta H° = -25.5$ kcal/mol, compared to a calculated value of −27.8 kcal/mol. Similarly for the $CH_3 + CH_2O$ reaction, the experimental $\Delta H° = -10.8$ kcal/mol, compared to a calculated value of −10.9 kcal/mol. The excellent agreement for the latter is fortuitous, since the calculated $\Delta H°$ is fairly sensitive to correlation corrections, possibly because the unpaired electron is on a carbon in the reactants but on an oxygen in the products. In both re-

(41) Pacansky, J.; Horne, D. E.; Gardini, G. P.; Bargon, J. *J. Phys. Chem.* **1977**, *81*, 2149.
(42) Saebø, S.; Radom, L.; Schaefer, H. F. *J. Chem. Phys.* **1983**, *78*, 845.
(43) *J. Phys. Chem. Ref. Data, Suppl.* **1985**, *14*(1).
(44) Castelhano, A. L.; Griller, D. *J. Am. Chem. Soc.* **1982**, *104*, 3655.

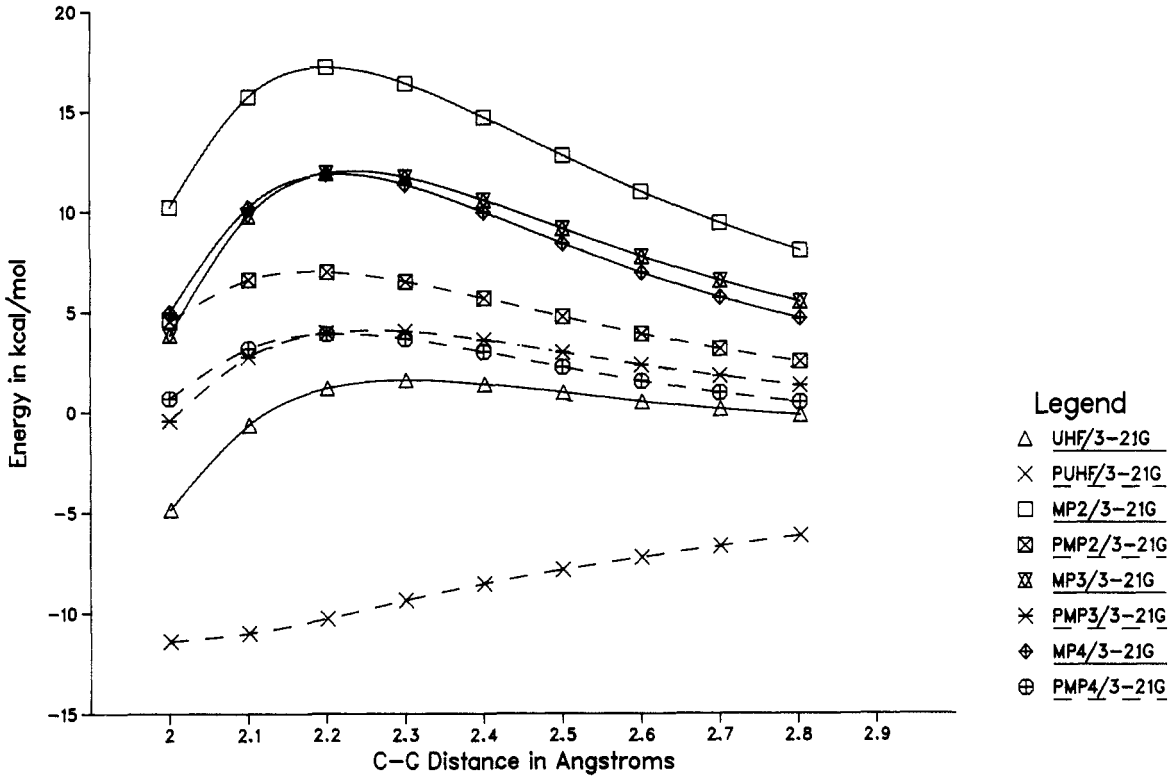

Figure 5. Potential energy profile along an approximate reaction path for methyl radical addition to formaldehyde computed with the 3-21G basis set.

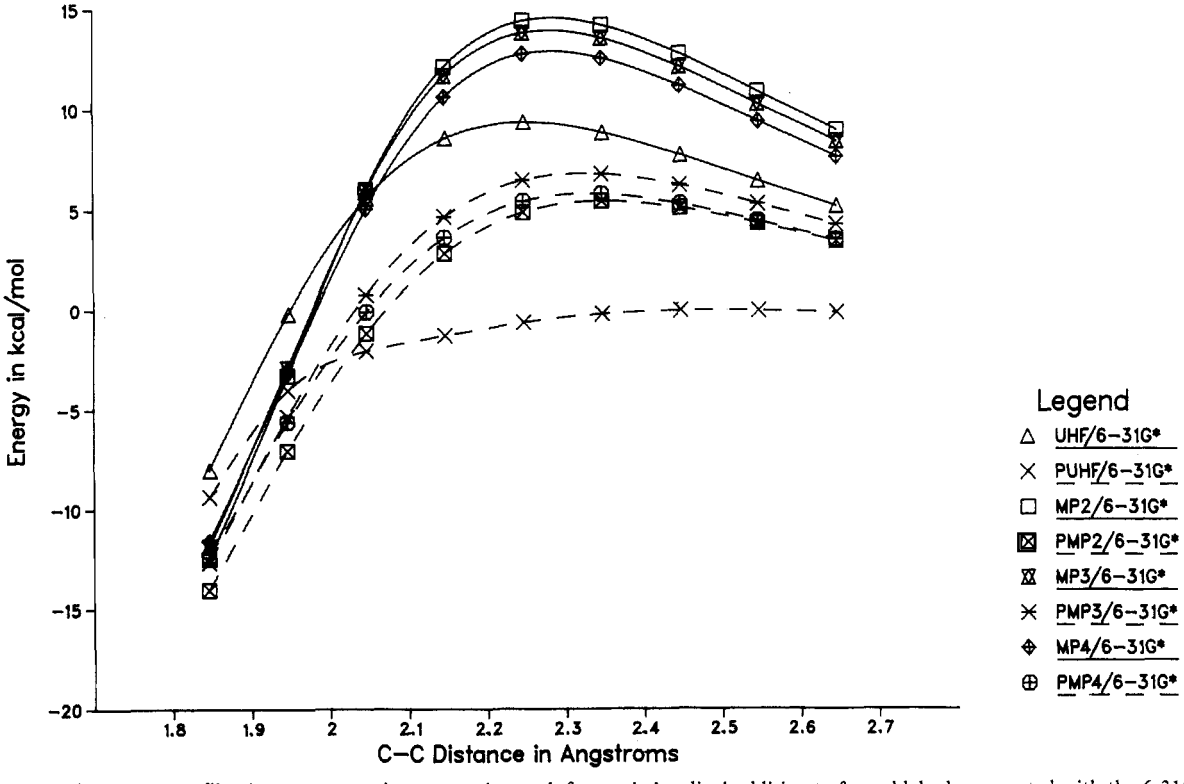

Figure 6. Potential energy profile along an approximate reaction path for methyl radical addition to formaldehyde computed with the 6-31G* basis set.

actions, the effect of spin projection on the heat of reaction is negligible.

Conclusions

Analogous to the radical plus multiple-bond reactions studied previously,[26] the barrier heights for methyl addition to ethylene and formaldehyde are affected significantly by spin projection. Barrier heights calculated by spin-unrestricted many-body perturbation theory can be in error by 5–10 kcal/mol due to spin contamination in the transition state. Similar size errors in barrier heights can be expected for other reactions with comparable degrees of spin contamination in the transition states.

Acknowledgment. This work was supported by a grant from the National Science Foundation (CHE 87-11901). We thank the Computer Services Center at Wayne State University for a generous alloction of computer time.

Registry No. CH_3, 2229-07-4; C_2H_4, 74-85-1; CH_2O, 50-00-0; C_3H_7, 2143-61-5; C_2H_5O, 2154-50-9.